

SUPPORTING INFORMATION

Long-range ferromagnetic exchange interactions mediated by Mn-Ce^{IV}-Mn superexchange involving empty 4*f* orbitals

Sayak Das Gupta,^a Robert L. Stewart,^b Dian-Teng Chen,^c Khalil A. Abboud,^a Hai-Ping Cheng,^c Stephen Hill,^b and George Christou^{a *}

^a Department of Chemistry, University of Florida, Gainesville, Florida 32611, USA

^b National High Magnetic Field Laboratory and Department of Physics, Florida State University, Tallahassee, Florida 32310, USA

^c Department of Physics, University of Florida, Gainesville, Florida 32611, USA

*E-mail for G.C.: christou@chem.ufl.edu

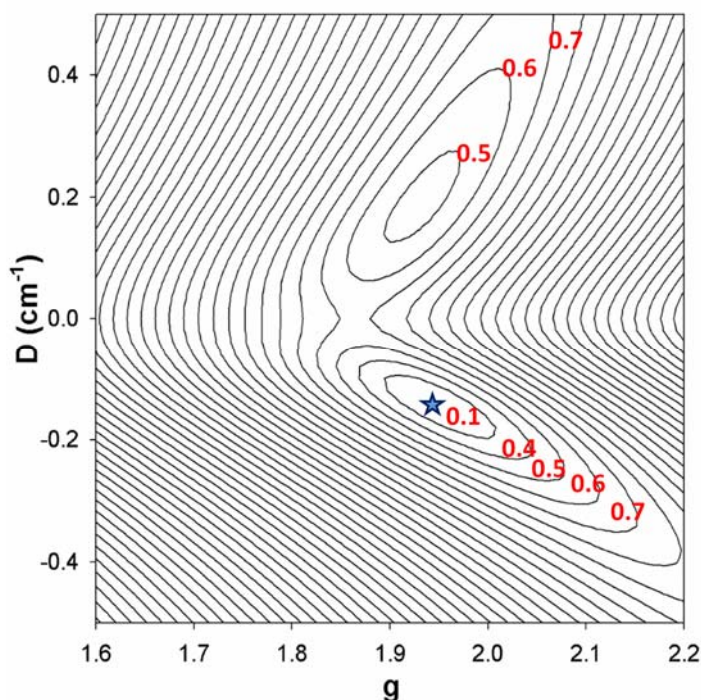


Figure S1. Root-mean-square g vs D error surface as a 2-D contour plot for the fit of $M/N\mu_B$ vs H/T data for complex **1**. The asterisk indicates the best-fit minimum corresponding to the fit parameters in the text.

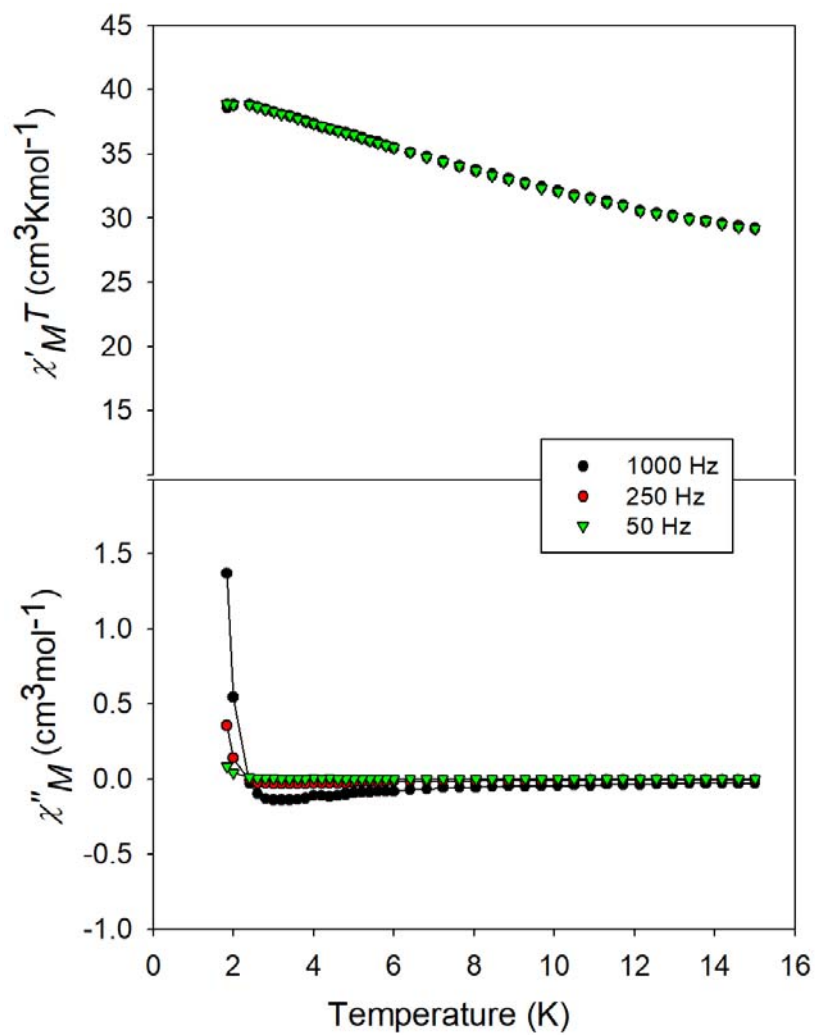


Figure S2. (top) ac in-phase $\chi'_M T$ vs T for complex **1** in a 3.5 G ac field at the indicated oscillation frequencies. **(bottom)** ac out-of-phase χ''_M vs T for **1** showing a weak tail due to onset of slow relaxation. The solid lines are guides for the eye.

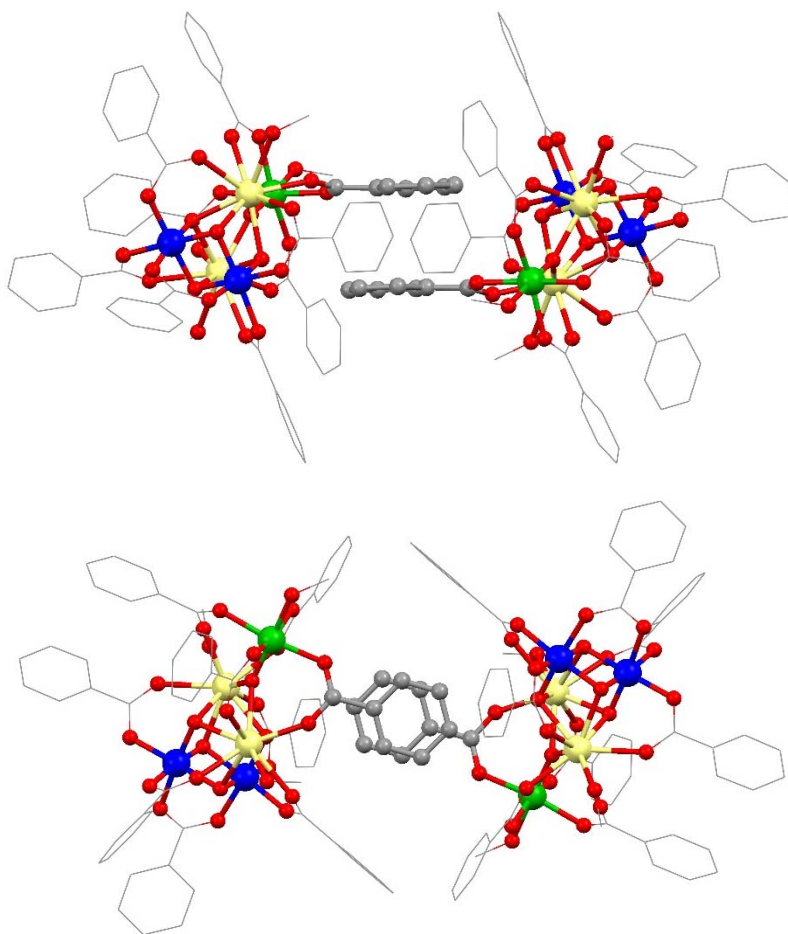


Figure S3. The π - π stacking between benzoate Ph rings on adjacent molecules of **2** from a side-view (**top**) and a top-view (**bottom**). The distance between the two rings is 3.49 Å

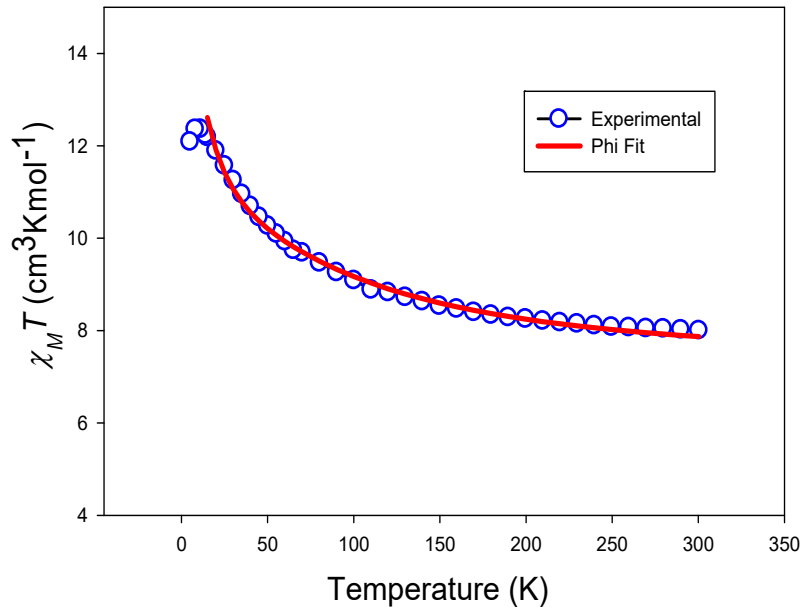


Figure S4. PHI fit for the dc $\chi_M T$ vs T data of complex **2**. See the text for the fit parameters.

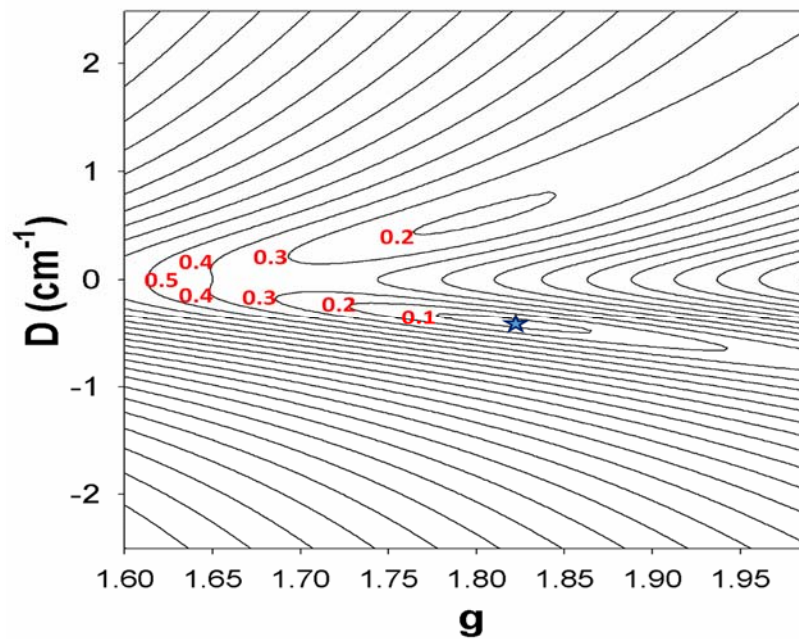


Figure S5. Root-mean-square D vs g fit error surface as a 2-D contour plot for the fit of $M/N\mu_B$ vs H/T data of complex **2**. The asterisk indicates the best-fit minimum corresponding to the fit parameters in the text.

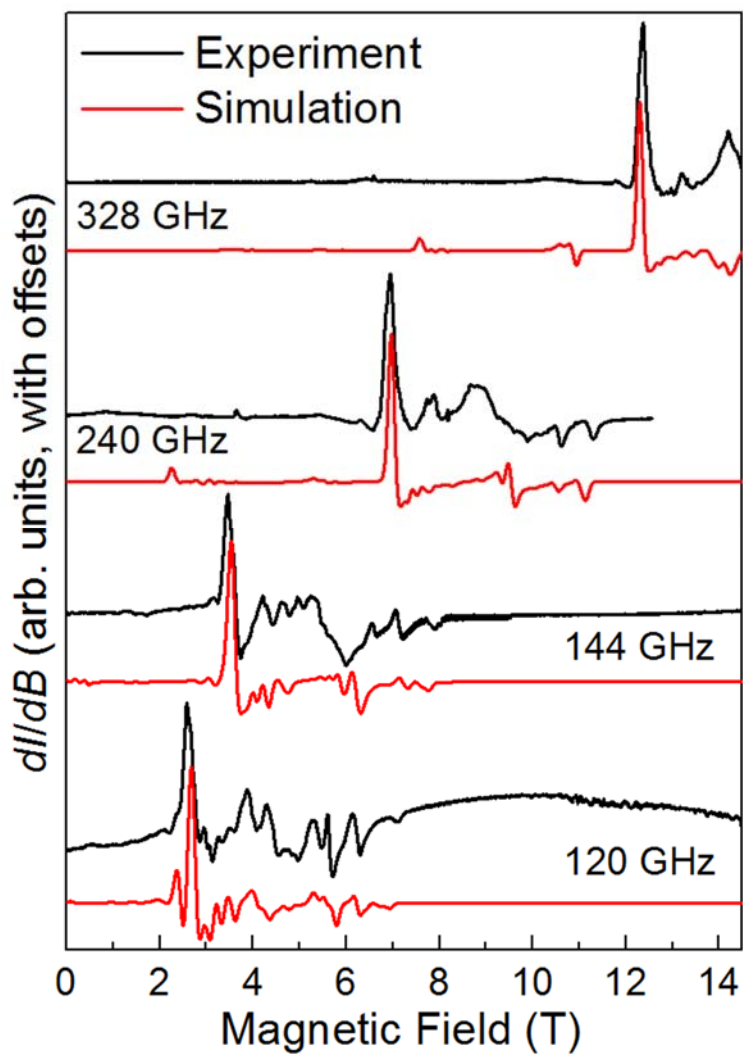


Figure S6. Variable-frequency powder HFEPR spectra for **1** (black lines) recorded at a temperature of 5 K, along with spectral simulations (red lines) generated using eq. 6 along with the parameters given in the main text.

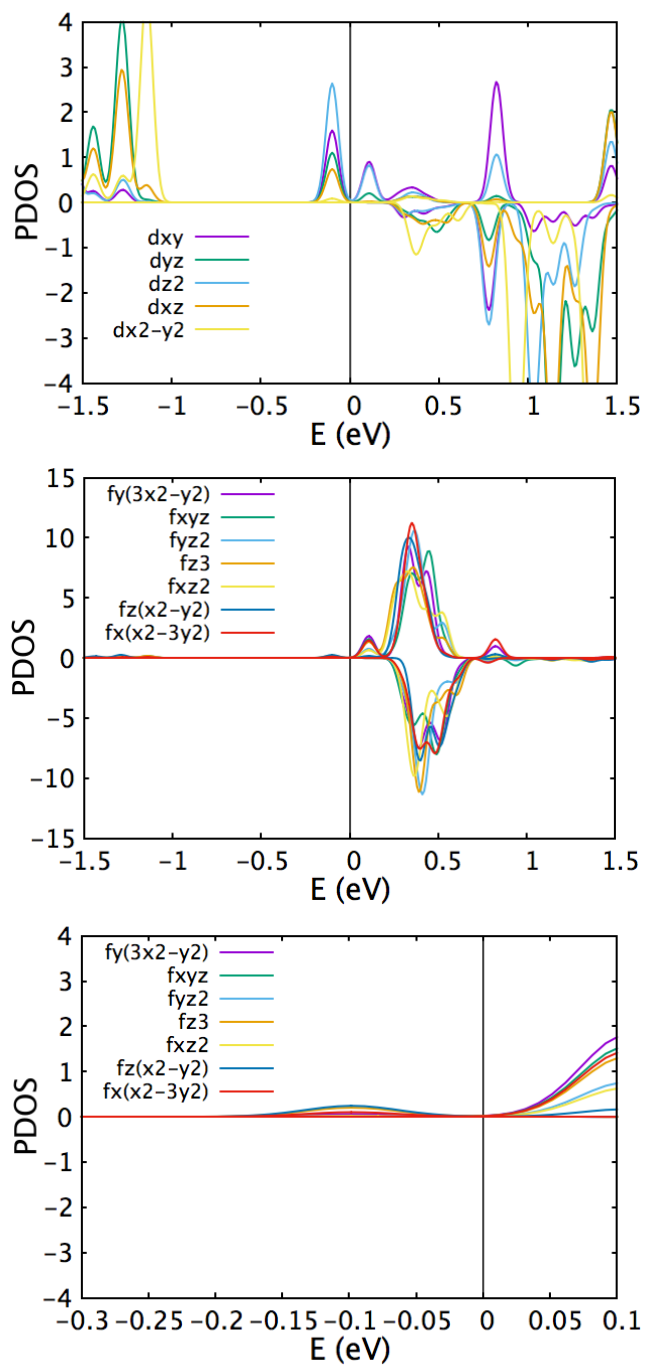


Figure S7. Projected density of states (PDOS) of the (top) Mn-*d* and (middle) Ce-*f* orbitals of complex **2**; (bottom) Expansion of the small component of Ce-*f* orbitals at -0.1 eV.

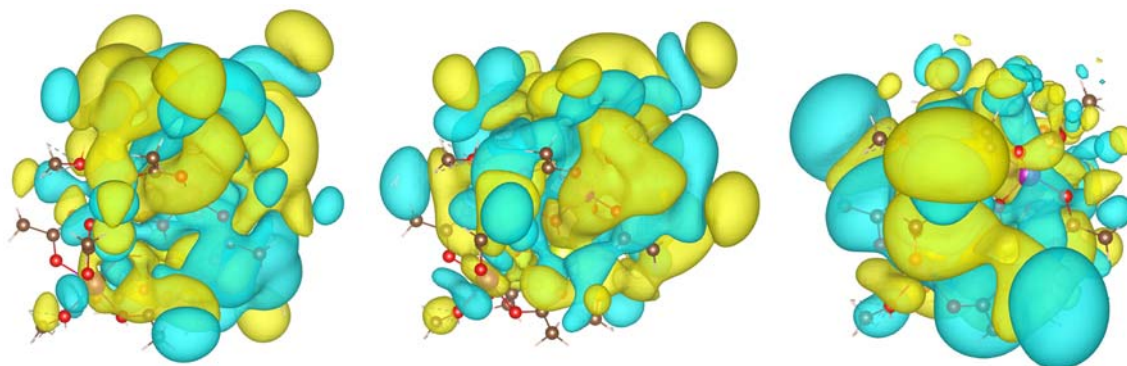


Figure S8. Wannier functions projected to Mn- d_z^2 orbitals for complex **2**. The first Wannier orbital has the largest spread of 4.37 \AA^2 .

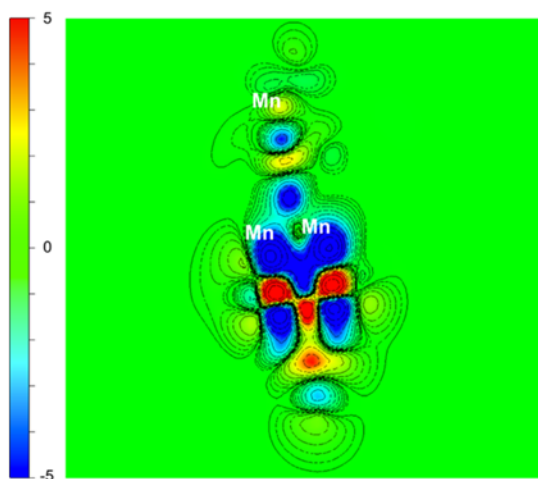


Figure S9. Cross-sectional contour plot, in units of $0.00827 \text{ \AA}^{-3/2}$, of a plane through three Mn ions in the Wannier function in Fig. S8 for complex **2** with the largest spread.

Table S1. Selected Interatomic Distances (Å) and Angles (deg) for Complex **1**

| | | | |
|---------------|------------|-------------------|------------|
| Ce(1)···Mn(2) | 3.225(8) | Mn(2)-O(4) | 1.821(5) |
| Ce(1)···Mn(1) | 3.282(8) | Mn(2)-O(10) | 1.909(4) |
| Ce(2)···Mn(5) | 3.216(6) | Mn(2)-O(5) | 1.812(5) |
| Ce(2)···Mn(4) | 3.294(1) | Mn(2)-O(4) | 1.821(5) |
| Ce(3)···Mn(5) | 3.291(9) | Mn(2)-O(10) | 1.909(4) |
| Ce(3)···Mn(4) | 3.313(1) | Mn(3)-O(5) | 1.891(5) |
| Mn(1)···Mn(2) | 2.943(9) | Mn(3)-O(10) | 2.457(5) |
| Mn(2)···Mn(3) | 3.025(7) | Mn(4)-O(2) | 1.837(4) |
| Mn(4)···Mn(5) | 2.737(9) | Mn(4)-O(7) | 1.850(5) |
| Ce(1)-O(3) | 2.234(4) | Mn(4)-O(8) | 1.852(4) |
| Ce(1)-O(5) | 2.314(4) | Mn(5)-O(6) | 1.828(4) |
| Ce(1)-O(4) | 2.333(5) | Mn(5)-O(7) | 1.848(5) |
| Ce(1)-O(1) | 2.413(4) | Mn(5)-O(8) | 1.855(5) |
| Ce(1)-O(2) | 2.482(4) | | |
| Ce(2)-O(6) | 2.255(4) | | |
| Ce(2)-O(1) | 2.323(4) | Mn(2)-O(10)-Mn(1) | 87.89(18) |
| Ce(2)-O(7) | 2.333(4) | Mn(2)-O(10)-Mn(3) | 86.77(17) |
| Ce(2)-O(2) | 2.411(5) | Mn(1)-O(10)-Mn(3) | 120.81(19) |
| Ce(2)-Mn(5) | 3.2156(11) | Mn(5)-O(7)-Mn(4) | 95.5(2) |
| Ce(2)-Mn(4) | 3.2941(11) | Mn(2)-O(5)-Mn(3) | 109.5(2) |
| Ce(3)-O(3) | 2.189(4) | Mn(5)-O(7)-Mn(4) | 95.5(2) |
| Ce(3)-O(8) | 2.365(4) | Mn(2)-O(4)-Mn(1) | 105.2(2) |
| Ce(3)-O(6) | 2.368(5) | Mn(4)-O(8)-Mn(5) | 95.2(2) |
| Ce(3)-O(2) | 2.417(4) | Mn(1)-Mn(2)-Mn(3) | 88.01(4) |
| Ce(3)-O(1) | 2.513(4) | Mn(2)-Mn(1)-Mn(3) | 46.80(9) |
| Mn(1)-O(3) | 1.863(5) | Mn(1)-Mn(3)-Mn(2) | 45.18(4) |
| Mn(1)-O(4) | 1.882(4) | Mn(1)-Mn(2)-Mn(3) | 88.01(4) |
| Mn(1)-O(24) | 1.915(4) | Mn(2)-O(4)-Mn(1) | 105.2(2) |
| Mn(1)-O(9) | 2.212(6) | Mn(5)-O(7)-Mn(4) | 95.5(2) |
| Mn(1)-O(10) | 2.311(5) | Mn(4)-O(8)-Mn(5) | 95.2(2) |
| Mn(2)-O(5) | 1.812(5) | | |

Table S2. Bond Valence Sums for Ce, Mn and O atoms in **1**

| atom^a | Ce^{III} | Ce^{IV} | | atom | BVS | assgnmt |
|-------------------------|-------------------------|-------------------------|------------------------|-------------|------------|------------------|
| Ce1 | 4.43 | <u>3.90</u> | | O1 | 1.90 | O ²⁻ |
| Ce2 | 4.35 | <u>3.83</u> | | O2 | 1.90 | O ²⁻ |
| Ce3 | 4.45 | <u>3.92</u> | | O3 | 2.05 | O ²⁻ |
| | | | | O4 | 1.98 | O ²⁻ |
| atom^a | Mn^{II} | Mn^{III} | Mn^{IV} | O5 | 2.01 | O ²⁻ |
| Mn1 | 3.24 | <u>2.97</u> | 3.12 | O6 | 1.85 | O ²⁻ |
| Mn2 | 4.32 | 3.96 | <u>4.15</u> | O7 | 2.02 | O ²⁻ |
| Mn3 | 3.21 | <u>2.94</u> | 3.09 | O8 | 1.96 | O ²⁻ |
| Mn4 | 4.32 | 3.95 | <u>4.15</u> | O9 | 1.05 | MeOH |
| Mn5 | 4.26 | 3.90 | <u>4.10</u> | O10 | 1.78 | MeO ⁻ |

^a For Ce and Mn, the metal oxidation state is the nearest integer to the underlined value, which is the closest to the charge for which it was calculated. For O, values in the ~1.8-2.0, ~1.0-1.2, and ~0.2-0.4 ranges indicate non-, single-, and double-protonation, respectively.

Table S3. Selected Interatomic Distances (Å) and Angles (deg) for Complex **2**

| | | | |
|---------------|----------|------------------|------------|
| Ce(1)···Mn(2) | 3.290(4) | Mn(2)-O(4) | 1.849(2) |
| Ce(1)···Mn(1) | 3.298(6) | Mn(2)-O(5) | 1.860(3) |
| Ce(1)···Ce(2) | 3.477(9) | Mn(3)-O(3) | 1.803(3) |
| Ce(2)···Mn(1) | 3.273(6) | Mn(3)-O(26) | 2.002(3) |
| Ce(2)···Mn(2) | 3.302(7) | | |
| Mn(1)-Mn(2) | 2.713(7) | Mn(1)-O(1)-Ce(2) | 104.55(11) |
| Ce(1)-O(3) | 2.308(2) | Mn(1)-O(1)-Ce(1) | 104.69(11) |
| Ce(1)-O(2) | 2.312(2) | Mn(2)-O(2)-Ce(1) | 105.17(11) |
| Ce(1)-O(1) | 2.328(2) | Mn(2)-O(2)-Ce(2) | 104.31(11) |
| Ce(1)-O(4) | 2.402(2) | Ce(1)-O(2)-Ce(2) | 96.53(8) |
| Ce(1)-O(24) | 2.558(3) | Mn(3)-O(3)-Ce(2) | 130.65(13) |
| Ce(2)-O(3) | 2.282(3) | Mn(3)-O(3)-Ce(1) | 130.77(13) |
| Ce(2)-O(1) | 2.302(2) | Ce(2)-O(3)-Ce(1) | 98.49(9) |
| Ce(2)-O(2) | 2.347(2) | Mn(1)-O(4)-Mn(2) | 94.41(11) |
| Ce(2)-O(5) | 2.380(2) | Mn(1)-O(4)-Ce(1) | 100.99(10) |
| Ce(2)-O(25) | 2.590(3) | Mn(2)-O(4)-Ce(1) | 100.62(10) |
| Mn(1)-O(1) | 1.818(2) | Mn(2)-O(5)-Mn(1) | 93.52(11) |
| Mn(1)-O(4) | 1.847(2) | Mn(2)-O(5)-Ce(2) | 101.58(11) |
| Mn(1)-O(5) | 1.863(2) | Mn(1)-O(5)-Ce(2) | 100.22(10) |
| Mn(2)-O(2) | 1.813(2) | | |

Table S4. Bond Valence Sums for Ce, Mn and O atoms in **2**

| atom | Ce ^{III} | Ce ^{IV} | atom | BVS | assignment | |
|------|-------------------|-------------------|------------------|------|-----------------|-----------------|
| Ce1 | 4.35 | <u>3.83</u> | O1 | 1.85 | O ²⁻ | |
| Ce2 | 4.39 | <u>3.87</u> | O2 | 1.82 | O ²⁻ | |
| | | | O3 | 1.90 | O ²⁻ | |
| atom | Mn ^{II} | Mn ^{III} | Mn ^{IV} | | | |
| Mn1 | 4.27 | 3.92 | <u>4.11</u> | O4 | 1.93 | O ²⁻ |
| Mn2 | 4.19 | 3.83 | <u>4.03</u> | O5 | 1.91 | O ²⁻ |
| Mn3 | 3.17 | <u>2.90</u> | 3.04 | O24 | 1.15 | MeOH |
| | | | | O25 | 1.27 | MeOH |
| | | | | O26 | 1.31 | MeOH |

^a For Ce and Mn, the metal oxidation state is the nearest integer to the underlined value, which is the closest to the charge for which it was calculated. For O, values in the ~1.8-2.0, ~1.0-1.2, and ~0.2-0.4 indicate non-, single-, and double-protonation, respectively.

Table S5. Calculated energies for different spin states for complex **1**

| Spin order (21345) ^a | Energy (Mn U = 0 eV) (meV) | Energy (Mn U = 4.4 eV) (meV) | Magnetic moment (μ_B) |
|------------------------------------|----------------------------------|------------------------------------|-----------------------------------|
| uuuuu | 0 | 0 | 17 |
| ddduu | 3 | 6 | -5 |
| dduuu | 29 | 90 | 1 |
| udddu | 25 | 79 | -3 |
| udduu | 6 | 43 | 3 |
| ududu | 2 | 70 | 3 |
| uduud | 4 | 73 | 3 |
| duddd | -16 | 35 | -9 |
| duduu | -18 | 33 | 3 |
| duudu | 23 | 78 | 3 |
| duuuu | 2 | 38 | 9 |
| uuddu | 50 | 126 | 5 |
| uudud | 48 | 125 | 5 |
| uuduu | 28 | 86 | 11 |
| uuudu | 20 | 40 | 11 |
| uuuud | 22 | 41 | 11 |

^a u = up, d = down; Mn atom numbering is that of Figure 1 – the two distant units are

Mn(1,2,3) and Mn(4,5)

VAN VLECK EQUATIONS

1) Van Vleck equation for fitting the dc data of complex 2

```
c=0.1250415518
k=0.695052552
m=-J1/k/T
n=-J2/k/T
TIP=0.0005
Num= +330.0*exp(m*-18.0+n*-12.0)
+180.0*exp(m*-8.0+n*-12.0)
+84.0*exp(m*0.0+n*-12.0)
+30.0*exp(m*6.0+n*-12.0)
+6.0*exp(m*10.0+n*-12.0)
+180.0*exp(m*-14.0+n*-6.0)
+84.0*exp(m*-6.0+n*-6.0)
+30.0*exp(m*0.0+n*-6.0)
+6.0*exp(m*4.0+n*-6.0)
+0.0*exp(m*6.0+n*-6.0)
+84.0*exp(m*-10.0+n*-2.0)
+30.0*exp(m*-4.0+n*-2.0)
+6.0*exp(m*0.0+n*-2.0)
+30.0*exp(m*-6.0+n*-0.0)
Deno= +11.0*exp(m*-18.0+n*-12.0)
+9.0*exp(m*-8.0+n*-12.0)
+7.0*exp(m*0.0+n*-12.0)
+5.0*exp(m*6.0+n*-12.0)
+3.0*exp(m*10.0+n*-12.0)
+9.0*exp(m*-14.0+n*-6.0)
+7.0*exp(m*-6.0+n*-6.0)
+5.0*exp(m*0.0+n*-6.0)
+3.0*exp(m*4.0+n*-6.0)
+1.0*exp(m*6.0+n*-6.0)
+7.0*exp(m*-10.0+n*-2.0)
+5.0*exp(m*-4.0+n*-2.0)
+3.0*exp(m*0.0+n*-2.0)
+5.0*exp(m*-6.0+n*-0.0)
;f=XM
f=((c*(g^2)/T)*(Num/Deno))+TIP
h=f*T
```

2) Van Vleck equation for fitting in-phase ac data of complex 1

```
c=0.1250415518
k=0.695052552
p=-J/k/T
m=-J/k/T
TIP=0.0008
N=+1453.5*exp(p*-80.75)+1020.0*exp(p*-63.75)+682.5*exp(p*-48.75)+429.0*exp(p*-35.75)+247.5*exp(p*-
24.75)+126.0*exp(p*-15.75)+52.5*exp(p*-8.75)

D=+18.0*exp(p*-80.75)+16.0*exp(p*-63.75)+14.0*exp(p*-48.75)+12.0*exp(p*-35.75)+10.0*exp(p*-
24.75)+8.0*exp(p*-15.75)+6.0*exp(p*-8.75)
;f=XM
f=((c*(g^2)/T)*(N/D))+TIP
h=f*T
```